Analysing the stability of graphene wrinkles using variational calculus

Jabr Aljedani[1] Michael J. Chen[2] Barry J. Cox[3]

(Received 27 January 2022; revised 24 June 2022)

Abstract

The chemical vapour deposition method is widely used to synthesise high quality graphene with a large surface area. However, the cooling process leads to the formations of ripples and wrinkles in the graphene structure. When a self-adhered wrinkle achieves the maximum height, it then folds onto the surface and leads to a collapsed wrinkle. The presence of such deformations often affects the properties of graphene. In this article, we describe a novel mathematical model to understand the formation and geometry of these wrinkles. The stability of these wrinkles is examined based on variational derivations for the energy of each structure. The model provides detailed explanations for the geometry of these wrinkles which would help in tuning their properties.

DOI:10.21914/anziamj.v63.17079, Published 2022-07-04, as part of the Proceedings of the 15th Biennial Engineering Mathematics and Applications Conference. ISSN 1445-8810. (Print two pages per sheet of paper.)

Contents

1 Introduction

Graphene consists of carbon atoms hexagonally arranged in a two-dimensional array. This structure has unique electronic, mechanical, and thermal properties [2, 5], which open doors for potential applications in many fields including engineering and biomedicine [6]. Graphene has been synthesised using various methods which can be classified into two broad approaches, the top-down approach and the bottom-up approach. In the top-down approach, graphene is derived from graphite, or multi-layer graphene, by enlarging the spacing distance between the graphene sheets in order to weaken the van der Waals (vdW) interaction energy. In the bottom-up approach, graphene is generated by building a block of carbon molecules. A well-known example for the bottom-up approach is chemical vapour deposition (CVD).

The CVD process involves epitaxial growth of graphene on a substrate at an elevated temperature [8]. During the cooling step, the differential thermal expansion of the graphene and the substrate leads to compressive forces on the graphene film. These forces lead to some graphene configurations including a ripple, an arch-shaped wrinkle, a standing self-adhered wrinkle (SAW) and a collapsed wrinkle (CW). These configurations alter the graphene electrical mobility [17], thermal conductivity [3, 11], and strain sensitivity [13]. Accordingly, understanding the formation of such configurations is essential to exploit the novel properties of folded graphene.

Table 1: Previous results for the transition height h_{tran}.

Study	substrate	h_{tran} (Å)
Experiment [7]	SiO_2/Si	50
Experiment [17]	SiO_2/Si	60
Experiment [10]	SiO_2/Si	101.5
Experiment [12]	Cu(111)	110
Theory [16]	ignored	69
Theory [12]	Cu(111)	76
Theory [17]	SiO_2/Si	84

A CW forms when a SAW folds towards the substrate after the maximum height is achieved. This maximum height of the SAW is the transition point between different graphene wrinkles, and hence it has been investigated both experimentally and theoretically. Experiments report values for this transition height from 50 to 110 Å, where theoretical works report values from 69 to 84 Å. These values depend on the materials of the substrate and they are summarised in Table 1. In this work, we utilise variational calculus to analyse the stability of graphene wrinkles. We use our model to predict numerical values for the transition length and height of SAW.

2 Modelling approach

We consider two configurations of graphene wrinkles, the SAW and the CW, as shown in Figure 1. Cox, Dyer, and Thamwattana [4] employed the calculus of variation to model the conformation of SAW (shown in Figure 1(a)), taking into account two energies, the bending elastic energy and the vdW interaction energy.

The elastic energy E_e is only considered in the regions where the graphene sheet bends, which for the SAW are the curves C_1 and C_2 in Figure 1(a). This energy is modelled by the integral of the square of the line curvature κ over the length of the bended region scaled by the bending rigidity of graphene γ.

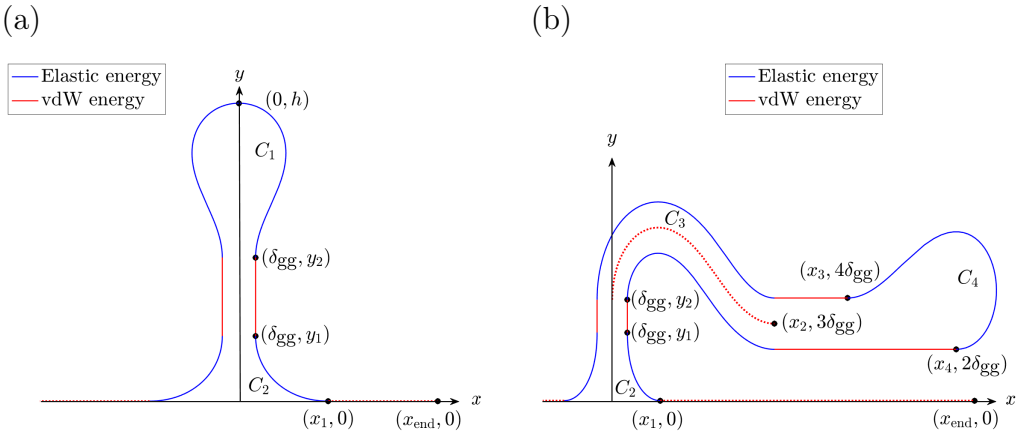

Figure 1: Representations for the geometry of graphene wrinkles, (a) a SAW, and (b) a CW.

The elastic energy of the SAW is mathematically modelled by the functional

$$E_e = 2\gamma \left(\int_{C_1} \kappa^2 \, ds + \int_{C_2} \kappa^2 \, ds \right),$$

where s is the arc length of the curve.

The vdW energy is only considered in the regions where a graphene layer becomes parallel to another graphene layer or to the substrate. This energy is modelled by multiplying the length of those regions by the strength of the vdW interaction energy. The vdW interaction energy for the SAW is

$$E_v = -\epsilon_{gs}(x_{end} - x_1) - \epsilon_{gg}(y_2 - y_1),$$

where ϵ_{gs} and ϵ_{gg} denote the graphene-substrate and graphene-graphene vdW interaction strengths, respectively.

A similar approach was taken by the present authors to model the more complicated configuration of the CW (shown in Figure 1(b)) [1]. We assume that both the SAW and CW have the same shape near where the wrinkle

attaches to the substrate, and so we name this curve C_2 in both wrinkles. The elastic energy is only considered in the bended regions, which in the CW configuration are curves C_2, C_3 and C_4. Hence, the bending elastic energy is the functional

$$E_e = \gamma \left(2 \int_{C_2} \kappa^2 \, ds + \int_{C_3} \kappa_{tot}^2 \, ds + \int_{C_4} \kappa^2 \, ds \right),$$

where κ_{tot} is the total squared curvatures of the two lines in the curve C_3. The vdW interaction energy of the CW is

$$\begin{aligned} E_v = &-\epsilon_{gs}(x_{end} - x_1) - \epsilon_{gg} \left[(y_2 - y_1) + \int_{C_3} ds \right] \\ &- \epsilon_{3gs}(x_3 - x_2) - \epsilon_{2gs}(x_4 - x_2), \end{aligned}$$

where ϵ_{Ngs} denotes the strength of the vdW interactions as N-layer graphene interacts with the substrate, for $N = 2, 3$. The distance $(y_2 - y_1)$ is introduced for modelling simplification, but we use $y_2 = y_1$ in the analysis to satisfy the physical condition of the CW.

This model involves a number of physical parameters relating to the interaction between graphene and the substrate. Here we apply this model to analyse the stability of graphene wrinkles located on a Cu(111) substrate and therefore the appropriate values for Cu(111) parameters are adopted by the model. These parameters are presented in Table 2. In our analysis, we adopt different values for the bending rigidity γ from the range given in Table 2.

The calculus of variations is employed to minimise the energy of each configuration. The approach relies on solving the Euler–Lagrange equation while applying the natural boundary conditions to obtain explicit formulae for the line curvature $\kappa(\theta)$ at each point (x, y) with a tangential angle θ measured from the positive direction of the x-axis. For $i \in \{1, \ldots, 4\}$, the obtained expression for line curvature $\kappa_{C_i}(\theta)$ of the curve C_i is utilised to:

- derive a parametric solution for the shape of the curve by solving the

Table 2: Numerical values for the parameters used in this model.

Parameter	Value	Source
γ (eV)	0.83–1.61	[14]
$2\delta_{gg}$ (Å)	3.34	[9]
ϵ_{gg} (eV/Å^2)	0.0214	[9]
ϵ_{gs} (eV/Å^2)	0.0132	[15]
ϵ_{2gs} (eV/Å^2)	0.0238	[1] (using LJ potential)
ϵ_{3gs} (eV/Å^2)	0.0243	[1] (using LJ potential)

pair of equations

$$x_{C_i} = \int_{C_i} \frac{\cos\theta}{\kappa_{C_i}(\theta)}\, d\theta\,, \quad y_{C_i} = \int_{C_i} \frac{\sin\theta}{\kappa_{C_i}(\theta)}\, d\theta\,;$$

- calculate the length of the curve by integrating ds over the length of that curve, that is

$$L_{C_i} = \int_{C_i} ds = \int_{C_i} \frac{d\theta}{\kappa_{C_i}(\theta)}\,;$$

- calculate the energy of the curve by integrating the squared curvature over the length of that curve multiplied by γ, that is

$$E_{C_i} = \gamma \int_{C_i} \kappa^2_{C_i}(\theta)\, ds = \gamma \int_{C_i} \kappa_{C_i}(\theta)\, d\theta\,.$$

We denote the total length of the wrinkle (the solid lines in Figure 1) by L_{tot} and the corresponding total energy by $E_{tot} = E_e + E_v$. For the SAW, the total length and total energy are, respectively,

$$L^s_{tot} = 2\,[L_{C_1} + (y_2 - y_1) + L_{C_2}]\,,$$
$$E^s_{tot} = 2\,(E_{C_1} + E_{C_2}) - \epsilon_{gg}(y_2 - y_1)\,.$$

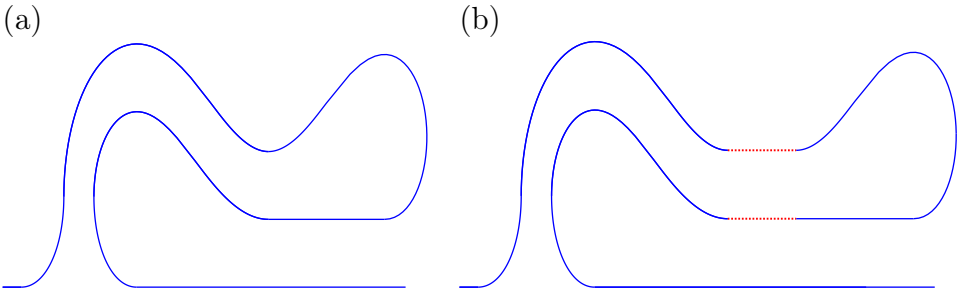

Figure 2: Representations for the geometry of: (a) CWA, and (b) CWB.

For the CW, the total length and total energy are, respectively,

$$L^c_{tot} = 2L_{C_2} + L_{C_3} + L_{C_4} + (x_3 - x_2) + (x_4 - x_2)\,, \tag{1}$$
$$E^c_{tot} = 2E_{C_2} + E_{C_3} + E_{C_4} - \epsilon_{3gs}(x_3 - x_2) - \epsilon_{2gs}(x_4 - x_2)\,. \tag{2}$$

3 Results

We now apply our model to consider two configurations for the CW which we name Collapsed wrinkle A (CWA) and Collapsed wrinkle B (CWB) and illustrate in Figure 2(a) and 2(b), respectively. The only difference between these configurations is the flat region following the folded bilayer (the curve C_3) seen in CWB but not in CWA. The two configurations are dependent on a competition between the elastic energy and the vdW interaction energy. The CWA maximises the elastic energy, while the CWB minimises the vdW interaction energy. The total length and energy are given by equations (1)–(2), but we set $x_2 = x_3$ for CWA.

Considering that the structure with minimum energy is energetically favourable, we account for the change in the total energy as the total length increases. The total length of CWA is increased by enlarging the folded bilayer section C_3. For CWB, the total length is increased by lengthening the flat region $(x_3 - x_2)$. The total energy E_{tot} is expressed in terms of the total length L_{tot} from which

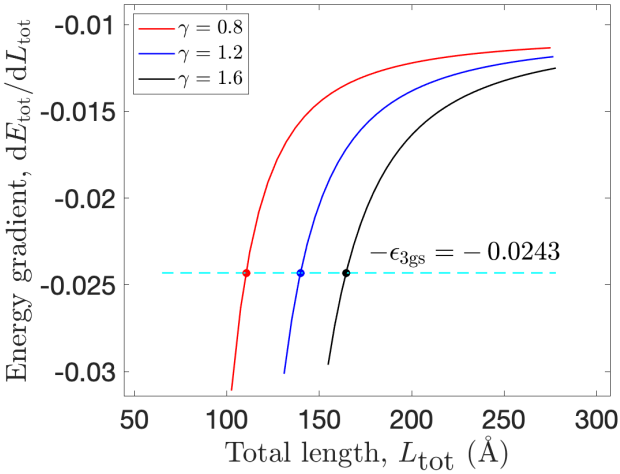

Figure 3: The gradients of the total energy E_{tot} with respect to the total length L_{tot}: CWA (solid curves), and CWB (the dashed curve).

the gradient of the curve is examined and representative plots are shown in Figure 3. The solid curves are the energy gradients of CWA which depend on the length of the curve C_3, while the horizontal dashed line is the energy gradient of CWB which is $-\epsilon_{3gs}$, the coefficient of x_3. The intersection points correspond to the lengths at which the CW starts producing the flat region. In other words, the intersection points indicate the transition length from CWA to CWB.

To obtain the length at which each configuration becomes stable, we perform an energy comparison between the SAW, CWA and CWB. The total length of the SAW is increased by lengthening the parallel region $(y_2 - y_1)$. The highlighted point in Figure 4, denotes the transition length and energy from SAW to CWB. The energy comparison also shows that CWA never occurs since there are always other structures with lower energies. However, CWA is utilised to obtain the starting length for CWB. Once the transition length

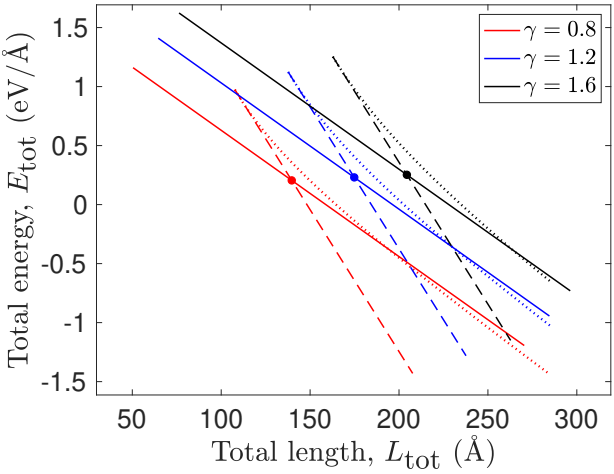

Figure 4: The total energy E_{tot} versus the total length L_{tot} for SAW (solid curves), CWA (dotted curves), and CWB (dashed curves), with the points indicating the transition lengths and energy from SAW to CWB.

Table 3: Values for L_{tran} and h_{tran} of graphene wrinkles on Cu(111) substrate.

γ (eV)	0.8	1.0	1.2	1.4	1.6	1.2 [12]
L_{tran} (Å)	143	158	175	190	207	—
h_{tran} (Å)	64.9	72.0	79.6	86.5	94.3	76.0

is determined, we then utilise the work by Cox, Dyer, and Thamwattana [4] to calculate the transition height at which the SAW folds over the substrate forming the CWB. Table 3 presents numerical values for the transition length and transition height obtained from this work for linearly spaced values of γ. For a bending rigidity $\gamma = 1.2$ eV, we obtain transition height $h_{tran} = 79.6$ Å which is consistent with the previous result of $h_{tran} = 76.0$ Å [12]. Finally, Figure 5 shows the predicted profiles of the CW on a Cu(111) substrate with transition length L_{tran} and different values of γ.

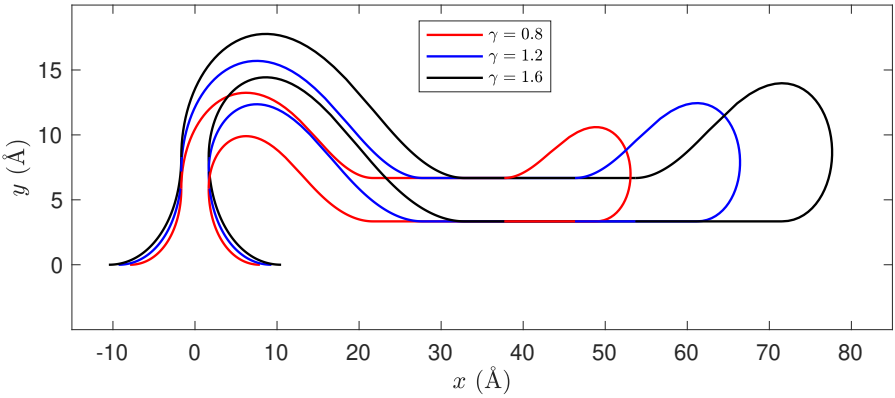

Figure 5: The obtained profiles for CWA with $L_{tot} = L_{tran}$, located on Cu(111) substrate.

4 Conclusion

This work provides theoretical analysis for the stability of graphene wrinkles. Mathematical models for graphene SAW and CW are utilised [4, 1]. The analysis is performed based on variational derivations for the energy of each configuration. Through an energy comparison, we find that the CW always contains a flat region between the curves C_3 and C_4. Utilising the work of Cox, Dyer, and Thamwattana [4], we also calculate the transition length and height of the SAW and obtain consistent values with reported measurements. The findings of this work enhance our knowledge of the geometry of these structures. This work may be extended to consider other substrates by applying the appropriate values for the parameters listed in Table 2.

References

[1] J. Aljedani, M. J. Chen, and B. J. Cox. "Variational model for collapsed graphene wrinkles". In: *Appl. Phys. A* 127.11, 886 (2021), pp. 1–13. DOI: 10.1007/s00339-021-05000-y. (Cit. on pp. C100, C102, C106).

[2] A. A. Balandin, S. Ghosh, W. Bao, I. Calizo, D. Teweldebrhan, F. Miao, and C. N. Lau. "Superior thermal conductivity of single-layer graphene". In: *Nano Lett.* 8.3 (2008), pp. 902–907. DOI: 10.1021/nl0731872. (Cit. on p. C98).

[3] S. Chen, Q. Li, Q. Zhang, Y. Qu, H. Ji, R. S. Ruoff, and W. Cai. "Thermal conductivity measurements of suspended graphene with and without wrinkles by micro-Raman mapping". In: *Nanotech.* 23.36, 365701 (2012). DOI: 10.1088/0957-4484/23/36/365701. (Cit. on p. C98).

[4] B. J. Cox, T. Dyer, and N. Thamwattana. "A variational model for conformation of graphene wrinkles formed on a shrinking solid metal substrate". In: *Mat. Res. Express* 7.8, 085001 (2020). DOI: 10.1088/2053-1591/abaa8f. (Cit. on pp. C99, C105, C106).

[5] A. K. Geim. "Graphene: Status and prospects". In: *Science* 324.5934 (2009), pp. 1530–1534. DOI: 10.1126/science.1158877. (Cit. on p. C98).

[6] K. Kostarelos and K. S. Novoselov. "Graphene devices for life". In: *Nature Nanotech.* 9 (2014), pp. 744–745. DOI: 10.1038/nnano.2014.224. (Cit. on p. C98).

[7] F. Long, P. Yasaei, R. Sanoj, W. Yao, P. Král, A. Salehi-Khojin, and R. Shahbazian-Yassar. "Characteristic work function variations of graphene line defects". In: *ACS Appl. Mat. Inter.* 8.28 (2016), pp. 18360–18366. DOI: 10.1021/acsami.6b04853. (Cit. on p. C99).

[8] R. Muñoz and C. Gómez-Aleixandre. "Review of CVD synthesis of graphene". In: *Chem. Vapor Dep.* 19.10–12 (2013), pp. 297–322. DOI: 10.1002/cvde.201300051. (Cit. on p. C98).

[9] L. Spanu, S. Sorella, and G. Galli. "Nature and strength of interlayer binding in graphite". In: *Phys. Rev. Lett.* 103.19, 196401 (2009). DOI: 10.1103/PhysRevLett.103.196401. (Cit. on p. C102).

[10] T. Verhagen, B. Pacakova, M. Bousa, U. Hübner, M. Kalbac, J. Vejpravova, and O. Frank. "Superlattice in collapsed graphene wrinkles". In: *Sci. Rep.* 9, 9972 (2019). DOI: 10.1038/s41598-019-46372-9. (Cit. on p. C99).

[11] C. Wang, Y. Liu, L. Li, and H. Tan. "Anisotropic thermal conductivity of graphene wrinkles". In: *Nanoscale* 6.11 (2014), pp. 5703–5707. DOI: 10.1039/C4NR00423J. (Cit. on p. C98).

[12] W. Wang, S. Yang, and A. Wang. "Observation of the unexpected morphology of graphene wrinkle on copper substrate". In: *Sci. Rep.* 7.1, 8244 (2017), pp. 1–6. DOI: 10.1038/s41598-017-08159-8. (Cit. on pp. C99, C105).

[13] Y. Wang, R. Yang, Z. Shi, L. Zhang, D. Shi, E. Wang, and G. Zhang. "Super-elastic graphene ripples for flexible strain sensors". In: *ACS Nano* 5.5 (2011), pp. 3645–3650. DOI: 10.1021/nn103523t. (Cit. on p. C98).

[14] Y. Wei, B. Wang, J. Wu, R. Yang, and M. L. Dunn. "Bending rigidity and Gaussian bending stiffness of single-layered graphene". In: *Nano Lett.* 13.1 (2013), pp. 26–30. DOI: 10.1021/nl303168w. (Cit. on p. C102).

[15] Z. Xu and M. J. Buehler. "Interface structure and mechanics between graphene and metal substrates: A first-principles study". In: *J. Phys.: Cond. Mat.* 22.48, 485301 (2010). DOI: 10.1088/0953-8984/22/48/485301. (Cit. on p. C102).

[16] Y. Zhang, N. Wei, J. Zhao, Y. Gong, and T. Rabczuk. "Quasi-analytical solution for the stable system of the multi-layer folded graphene wrinkles". In: *J. Appl. Phys.* 114.6, 063511 (2013). DOI: 10.1063/1.4817768. (Cit. on p. C99).

[17] W. Zhu, T. Low, V. Perebeinos, A. A. Bol, Y. Zhu, H. Yan, J. Tersoff, and P. Avouris. "Structure and electronic transport in graphene wrinkles". In: *Nano Lett.* 12.7 (2012), pp. 3431–3436. DOI: 10.1021/nl300563h. (Cit. on pp. C98, C99).

Author addresses

1. **Jabr Aljedani**, School of Mathematical Sciences, University of Adelaide, South Australia 5005, AUSTRALIA.
mailto:jabr.aljedani@adelaide.edu.au
orcid:0000-0002-8761-5870

2. **Michael J. Chen**, School of Mathematical Sciences, University of Adelaide, South Australia 5005, AUSTRALIA.
mailto:michael.chen@adelaide.edu.au
orcid:0000-0003-1855-7897

3. **Barry J. Cox**, School of Mathematical Sciences, University of Adelaide, South Australia 5005, AUSTRALIA.
mailto:barry.cox@adelaide.edu.au
orcid:0000-0002-0662-7037